Food Hydrocolloids 67 (2017) 130–138

Contents lists available at ScienceDirect

Food Hydrocolloids

journal homepage: www.elsevier.com/locate/foodhyd

Formation and colloidal stability of ovalbumin-retinol nanocomplexes

Flavia F. Visentini [a, b], Osvaldo E. Sponton [a, b], Adrián A. Perez [a, b], Liliana G. Santiago [b, *]

[a] Consejo Nacional de Investigaciones Científicas y Técnicas de la República Argentina, CONICET, Argentina
[b] Área de Biocoloides y Nanotecnología, Instituto de Tecnología de Alimentos, Facultad de Ingeniería Química, Universidad Nacional del Litoral, 1 de Mayo 3250, Santa Fe, 3000, Argentina

ARTICLE INFO

Article history:
Received 28 July 2016
Received in revised form
20 December 2016
Accepted 22 December 2016
Available online 26 December 2016

Keywords:
Retinol
Ovalbumin
Heat-induced nanoparticle
Nanocomplexes
Vehiculization
Photochemical stability

ABSTRACT

This work is aimed to obtain and characterize nanocomplexes formed by non-covalent attractive interactions between ovalbumin (OVA) and retinol (RET). In order to gain some ideas about the effect of OVA aggregation on RET complexation, OVA nanoparticles (OVAn) obtained by controlled heat treatment (85 °C, 5 min) were also evaluated. Nanocomplex formation was monitored by intrinsic and extrinsic fluorescence spectroscopy. Results suggest that OVA was more effective for binding RET than OVAn, possibly because aggregate formation could employ some hydrophobic patches needed for RET binding. Furthermore, nanocomplex colloidal stability was studied by means of absorbance (at 400 nm), particle size distribution (PSD) and ζ potential determinations. At pH values of common foods (4.0 and 7.0), nanocomplex colloidal stability mainly depended on aqueous phase behaviour of the proteins (OVA and OVAn). Finally, long-term photochemical stability against light and oxygen of RET nanocomplexes depended on solution pH and protein aggregation.

1. Introduction

Retinol (RET) or vitamin A is a fat-soluble compound critical for the correct performance of many biological processes including vision, fetal growth, immune response, cell differentiation and proliferation, and it plays an important role in different pathologies (Stephensen, 2001; Sun & Kawaguchi, 2011). It is the immediate precursor to two important active metabolites or retinoids: retinal, which plays a key role in vision; and retinoic acid, which serves as an intracellular messenger in gene transcription (Noy, 2000). Humans cannot synthesize it, so its intake must be performed through consumption of vegetables and fruits (e.g. sweet potatoes, carrots, dark leafy greens, winter squashes, lettuce, dried apricots, cantaloupe, bell peppers, fish, liver, and tropical fruits) rich in provitamin A carotenoids (Castenmiller & West, 1998).

RET deficiency cases are usually reported in developing countries, so that food fortification strategies should be implemented (Sommer & Davidson, 2002). However, RET incorporation into foods could present two disadvantages: (i) their poor solubility in water, which turn it generally incompatible with aqueous matrices, and (ii) their high sensitivity to light and oxygen, which leads to their photochemical decomposition, and consequently, to the deterioration of their biological properties (Allwood & Plein, 1986; Failloux, Bonnet, Perrier, & Baron, 2004; Vilanova & Solans, 2014). In order to solve these problems, several encapsulation technologies could be implemented, e.g. emulsions (Carlotti, Rossatto, & Gallarate, 2002), micelles (Blayo, Marchal, Lange, & Dumay, 2014), lipid solid nanoparticles (Jenning & Gohla, 2001), liposomes (Lee et al., 2002), polymer systems (Hwang, Oh, & Oh, 2005), etc. Nevertheless, these technologies have not been widely applied in food industry (Loveday & Singh, 2008).

The ability for binding lipophilic ligands that shows some globular proteins could be used as a strategy for introducing RET into food matrices. In this sense, the main milk whey protein, β-lactoglobulin (BLG), is the most recognized protein showing the ability for binding RET (Muresan, van der Bent, & de Wolf, 2001; Puyol, Perez, Ena, & Calvo, 1991). This ability is driven by non-covalent attractive forces, involving particular protein domains. BLG has two hydrophobic pockets that are potentially capable for binding lipophilic ligands: one in *calyx* formed by β-barrel, and the other one between α-helix and β-barrel surface. Although binding sites for ligands remain controversial, most evidence indicates that RET binds at the *calyx* (Kontopidis, Holt, & Sawyer, 2002; Wang, Allen, & Swaisgood, 1999). Finally, it was demonstrated that the BLG-RET complexes formation promoted a considerable RET protection against heat, oxidation and UV radiation (Hattori, Watabe, &

* Corresponding author.
E-mail address: lsanti@fiq.unl.edu.ar (L.G. Santiago).

http://dx.doi.org/10.1016/j.foodhyd.2016.12.027
0268-005X/

Takahashi, 1995; Shimoyamada, Yoshimura, Tomida & Watanabe, 1996).

In order to extend the application of RET vehiculization strategies based on protein-ligand complexes, the current research should be focused to the evaluation of other food globular proteins. In this sense, the main protein of egg white protein (EWP), ovalbumin (OVA), could be used because of its great availability in the agro-food sector. OVA is a monomeric protein of 43 KDa, and it has 4 sulfhydryl groups (-SH) and one disulfide bond (S-S) per monomer (Weijers & Visschers, 2002). It is constituted of 385 amino-acids, from which a half is hydrophobic and mainly buried into the protein structure and a third are charged aminoacids (Nisbet, Saundry, Moir, Fothergill, & Fothergill, 1981). The OVA properties to bind hydrophobic ligand have been poorly studied; furthermore, OVA ability to bind RET is not known at the present. According to this, the aim of the present paper was to study the obtention of nanocomplexes formed by non-covalent attractive interactions between RET and OVA. Moreover, because of heat-induced protein aggregates are often produced in food processing (Croguennec, Renault, Beaufils, Dubois, & Pezennec, 2007; Le Maux, Bouhallab, Giblin, Brodkorb, & Croguennec, 2013; Perez, Andermatten, Rubiolo, & Santiago, 2014; Sponton, Perez, Carrara, & Santiago, 2015a; Sponton, Perez, Carrara, & Santiago, 2015b), this research was extended to the evaluation of nanosized heat-induced OVA aggregate (OVAn) previously characterized in our lab (Sponton et al. 2015b). In recent papers, the ability of OVAn for binding a model hydrophobic ligand, linoleic acid (LA), was highlighted (Sponton et al., 2015a, 2015b, Sponton, Perez, Carrara, & Santiago, 2016). Hence, OVAn could be assayed for knowing the effect of controlled heat treatment on OVA ability to bind RET. For predicting the nanocomplex colloidal stability at pH values of common foods, particle size and ζ potential measurements were performed. Finally, the photochemical stability of RET nanocomplexes was also examined.

2. Materials and methods

2.1. Materials

Native ovalbumin (OVA, product A5503, purity 98% according to agarose gel electrophoresis) was purchased from Sigma (USA). Ovalbumin heat-induced nanoparticle (OVAn) was produced according to Sponton et al. (2015b). Briefly, OVA dispersion was prepared at 10 g/L, 50 mM NaCl and pH was adjusted 7.5 by using 0.1 M NaOH. Then, 2 mL aliquots were dispensed in glass tubes and were heated in a water bath at 85 °C for 5 min. Subsequently, tubes were removed and immediately cooled in an ice bath. Tubes containing OVAn were kept at 4 °C until further analysis. Retinol (RET, product 17772, purity ≥95.0% according to HPLC) was also obtained from Sigma (USA). RET was kept in darkness under N_2 atmosphere at −20 °C according to manufacturer advice. Fluorescence probe 1-anilino-8-naphthalene sulfonic acid (ANS) was purchased from Fluka Chemie AG (Switzerland). Additional analytical reagents were supplied from Cicarelli (Argentina).

2.2. Protein-retinol complexes formation

2.2.1. Intrinsic fluorescence

Formation of OVA-RET and OVAn-RET complexes was monitored by intrinsic fluorescence spectroscopy. For this, OVA and OVAn were dispersed in phosphate buffer (pH 7, 50 mM) at 1 μM final protein concentration. On the other hand, a stock RET solution was prepared at 20 mM concentration in ethanol. Then, 3 mL of protein (OVA or OVAn) dispersion was titrated with increasing volumes (0–30 μl) of stock RET solution. It is important to remark that final ethanol concentration in mixed systems was lower than 1 vol%; therefore, it could be assumed that no protein structural modifications were induced (Cogan, Kopelman, & Shinitzky, 1976). Protein-RET complexes dispersions were stored in darkness for 2 h for reaching equilibrium. Intrinsic fluorescence experiments were performed in a Hitachi F-2000 spectrophotometer (Japan) exciting at 280 nm (Trp and Tyr excitation), and registering emission spectra between 300 and 425 nm. Fluorescence intensity (FI) data were corrected by inner filter effect due to RET absorption at 250–400 nm, according to van de Weert and Stella (2011). Corrected FI (FI_{corr}) data for OVA-RET and OVAn-RET complexes were obtained as following:

$$FI_{corr} = FI_{obs} \times 10^{\frac{A_{ex}d_{ex}}{2} + \frac{A_{em}d_{em}}{2}} \quad (1)$$

where FI_{obs} is the observed fluorescence intensity, A_{ex} and A_{em} are the measured change in absorbance value at the excitation and emission wavelength, respectively, caused by ligand addition, and d_{ex} and d_{em} are the cuvette length (cm) in direction of excitation and emission, respectively. Absorption spectra for OVA-RET and OVAn-RET complexes were collected from 250 to 450 nm by using a Perkin Elmer Lambda 20 UV/Vis spectrophotometer (USA). The FI_{corr} values at the maximum emission wavelength were also expressed in terms of relative fluorescence intensity (RFI), being $RFI = FI/FI_0$, where FI is the intrinsic fluorescence intensity of protein-RET complexes and FI_0 corresponds to intrinsic fluorescence intensity of pure protein (OVA or OVAn) in solution (Perez et al., 2014; Sponton, Perez, Carrara, & Santiago, 2014). Usually, ligand addition to protein dispersions can produce increasing or decreasing RFI values, which would correspond to the formation of protein-ligand complexes in solution (Frapin, Dufour, & Haertle, 1993; Le Maux, Bouhallab, Giblin, Brodkorb, & Croguennec, 2013; Perez, Sponton, Andermatten, Rubiolo, & Santiago, 2015; Sponton et al., 2015b).

Furthermore, FI_{corr} data were used to calculate the binding parameters: stoichiometry or number of RET molecules bounds (n) and association constant (K_a). For this, modified Scatchard model was applied (Le Maux et al., 2013):

$$P_{total}(1 - f_i) = \frac{[RET]}{n}\left(\frac{1}{f_i} - 1\right) - \frac{1}{nK_a};\ f_i = \frac{FI_i - FI_0}{FI_{máx} - FI_0} \quad (2)$$

where P_{total} is the total protein (OVA or OVAn) concentration, RET is the retinol concentration, n is the number of RET molecules bound at protein saturation, K_a is the association constant, f_i is the fraction of one site of the protein occupied by the RET and FI_0, FI_{max} and FI_i are the fluorescence intensity initial, at saturation and at the ligand/protein ratio, respectively. It is important to remark that OVAn molar concentration was expressed in terms of native OVA monomeric unit (Sponton et al 2016). Fluorescence and absorption measurements were performed at room temperature (20 °C) in triplicate.

2.2.2. Extrinsic fluorescence

The binding mode of RET to proteins (OVA and OVAn) was examined by extrinsic fluorescence spectroscopy. Extrinsic experiments were conducted by using ANS as a fluorescent probe. Usually, ANS is bound to proteins by non-covalent attractive forces, mainly by hydrophobic interactions. OVA and OVAn were dispersed in phosphate buffer (pH 7, 50 mM) at 1 μM final protein concentration. Then, protein-RET complex dispersions were prepared as it was described previously. Subsequently, 9 μl of 15 mM ANS solution were added to each system (Perez, Carrera-Sanchez, Rodriguez-Patino, Rubiolo & Santiago, 2012). Extrinsic fluorescence emission spectra were obtained from 420 to 600 nm at 390 nm excitation

wavelength by using a Hitachi F-2000 spectrophotometer (Japan). Measurements were carried out at room temperature (20 °C) in triplicate. Extrinsic emission fluorescence values were expressed in terms of ANS relative fluorescence intensity (RFI_{ANS}), being $RFI_{ANS} = FI/FI_0$, where FI is the ANS emission fluorescence intensity of protein-RET complexes and FI_0 corresponds to ANS emission fluorescence intensity of pure protein (Sponton et al., 2016).

2.3. Complexes colloidal stability

2.3.1. Absorbance measurements

In this work, it was hypothesized that colloidal stability of protein-ligand complexes could be governed by protein phase behaviour at different pH values. According to this, OVA and OVAn dispersions were prepared as it was mentioned above, and the aqueous medium pH was decreased from 7.5 to 2.5 by using 1.0 M HCl. It was assumed pH changes did not alter significantly the ionic strength of protein dispersions. Absorbance at 400 nm was determined as soon as systems were prepared, and it was considered as a measure of system turbidity (Perez et al., 2015). Determinations were carried out in a Jenway 7305 spectrophotometer (UK). Subsequently, the protein dispersions at different pH values were kept in repose at room temperature (25 °C) and ζ potential measurements were performed as it will be described in the next section. Finally, dispersions visual appearance was registered after 24 h preparation by means of a photo camera (Cyber-shot 12.1 mpx, Sony, USA).

2.3.2. Particle size distribution and ζ potential

Particle Size Distribution (PSD) and ζ potential determinations were performed in a Zetasizer Nano ZS90 (Malvern Instruments Ltd., UK). PSD was obtained by dynamic light scattering (DLS) at a set angle of 90°. The light source of the instrument had been operated with a wavelength of 632.8 nm. Particle diameter was obtained from the peak of the Intensity (%) vs diameter (nm) curve (PSDi). PSD in Volume (%) (PSDv) was also considered in particle diameter analysis. PSDv was generated from PSDi by applying Mie theory. For ζ potential measurements, the instrument determined the electrophoretic mobility distribution of particles by mean of laser Doppler velocity technique. The ζ potential values were calculated according to Smoluchowski model by using the equipment software. All determinations were performed in triplicate at 25 °C.

2.4. Retinol photochemical decomposition assay

The effect of RET complexation on its photochemical decomposition in aqueous solution was evaluated according to Shimoyamada, Yoshimura, Tomida, & Watanabe, 1996. For this, RET photochemical decomposition was determined as a percentage of the initial absorbance at 330 nm (ABS_0) over 30 h examination. Thus, RET decomposition level was calculated as following:

$$RET\ \ Decomposition\ \ (\%) = \frac{ABS_0 - ABS_t}{ABS_0} \times 100\% \qquad (3)$$

where ABS_t is RET absorbance at a given time in the range of 0 and 30 h. Experiments were performed adding ethanolic RET solution to 3 mL of protein dispersion (OVA and OVAn) in glass tubes. These systems were placed at 35 cm (arbitrary position) under a compact fluorescent lamp (BAW, 65 W, 750 lm, 6400 K). Two kind of controls were also assayed: (i) pure RET solution kept in darkness, which was considered as a measure of RET photochemical decomposition due to the presence of dissolved oxygen (DO) in aqueous solution ($RET_{darkness}$), and (ii) pure RET solution kept under light exposition, which was considered as a measure of RET photochemical decomposition as a consequence of combined action of DO and light (RET_{light}). Experiments were conducted at room temperature (25 °C) in triplicate.

2.5. Dissolved oxygen determination

In order to perform a better discussion of results obtained in RET photochemical decomposition assay, dissolved oxygen (DO) concentration was determined. For this, DO was determined in systems without RET to know DO concentration at which RET would be exposed initially. Hence, the measurements were performed in phosphate buffer, OVA pH 4.0and pH 7.0, and OVAn pH 7.0 systems. Buffer solution without RET was also included as control. Standard iodometric test with azide modification was applied (Rice, Baird, Eaton, & Clesceri, 2012). Samples were placed in 250 mL Winkler frasks, 1 mL $MnSO_4$ solution was added, followed by 1 mL alkali-iodide-azide reagent. In order to exclude air bubbles, frasks were carefully capped and mixed by inverting a few times. Frasks remained in repose until precipitate was settled sufficiently. Then, 1 mL concentrated H_2SO_4 was added and mixed by inverting several times until dissolution was completed. A volume of 200 mL sample was titrated with 0.025 M $Na_2S_2O_3$ solution. Few drops of starch solution (as indicator) were added. Titration end point was considered at blue colour disappearance. For titration of 200 mL sample, 1 mL 0.025 M $Na_2S_2O_3$ is equivalent to 1 mg DO/L. Determinations were done at least in duplicate at room temperature (25 °C).

2.6. Statistical analysis

Statistical differences were determined through one way analysis of variance (ANOVA) using StatGraphics Plus 3.0 software. For this, LSD test at 95% confidence level was applied.

3. Results and discussion

3.1. Protein-retinol complexes formation

3.1.1. Intrinsic fluorescence

In this study, complexes formation was studied monitoring the changes in intrinsic fluorescence intensity after RET addition to protein (OVA and OVAn) dispersions. Protein-RET complexes formation could respond to a process in which binding sites on protein are gradually saturated by RET molecules. In order to confirm this assumption, the effect of RET concentration (0–200 μM) on the intrinsic fluorescence emission for OVA and OVAn was evaluated, and results are shown in Fig. 1a and c, respectively. From these spectra, RFI values were obtained, and they were also included in Fig. 1b and d. It can be deduced that:

(i) For OVA, the increase in RET concentration caused an increase in FI, and no shifts at the maximum emission wavelength were detected (Fig. 1a). This behaviour is better observed considering RFI values in Fig. 1b. According protein primary structure, OVA has three Trp residues and ten Tyr residues (Nisbet et al., 1981), so the registered intrinsic fluorescence should be considered as an average of emission contributions. The results could be explained considering that RET is bound at OVA domains far away from Trp and/or Tyr residues, which could induce slight protein conformational changes (Frapin et al., 1993; Wang et al., 1999). Similar fluorescence behaviours were observed for the binding of fatty acids to BLG (Le Maux et al., 2013; Perez et al., 2014; Sponton et al., 2014). Moreover, it was observed that RFI

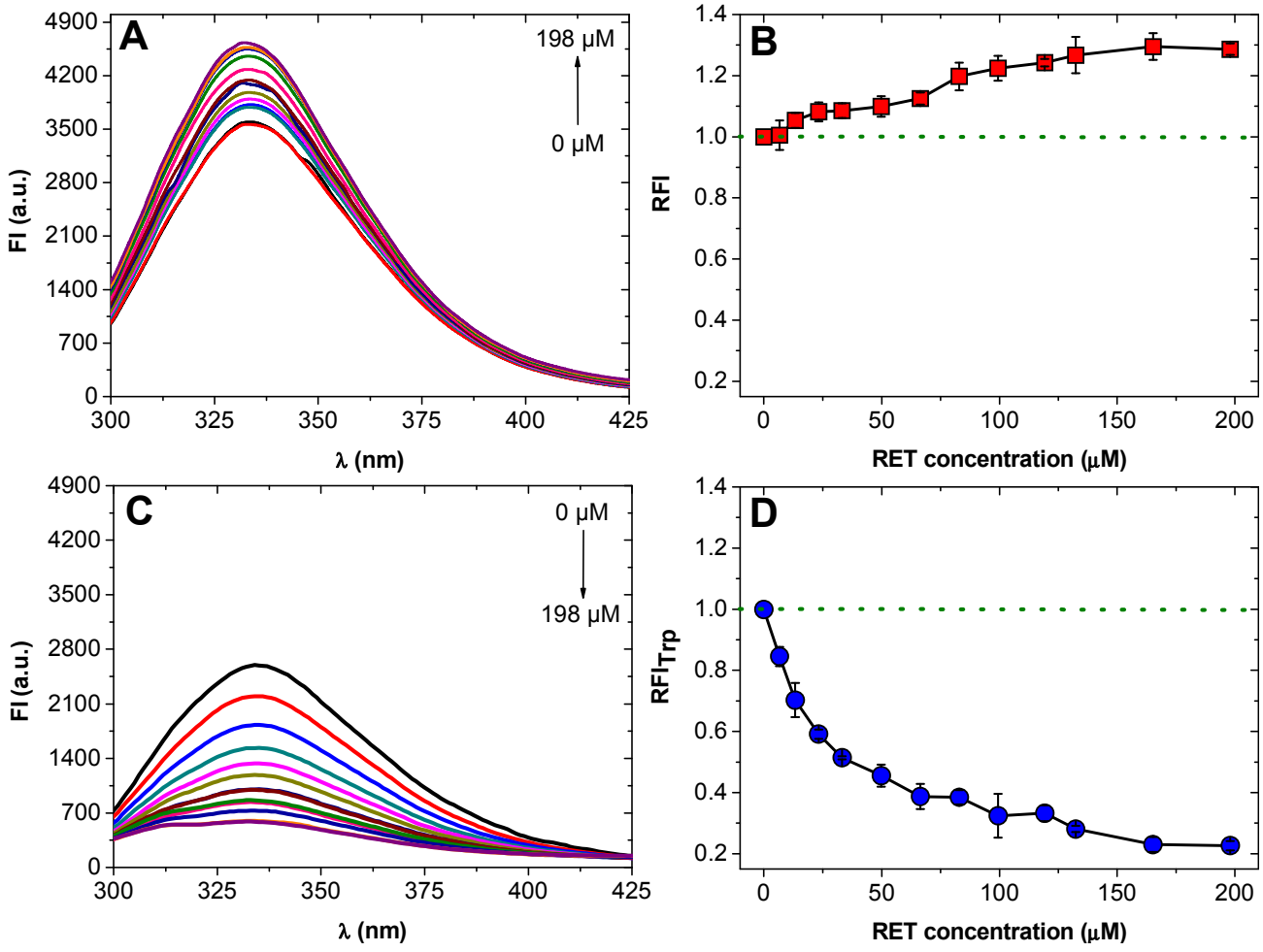

Fig. 1. Effect of retinol (RET) concentration (in the range 0–198 μM) on the Intrinsic fluorescence intensity (FI) for OVA (A) and OVAn (C); and on the Trp relative fluorescence intensity (RFI) for (■) OVA (B), and (●) OVAn (D). Conditions: Protein concentration: 1 μM, pH 7.0 (50 mM phosphate buffer), Temperature: 20 °C. Values are showed as mean ± standard deviation.

values increased reaching a *plateau* at approximately 100 μM RET, which could indicate the saturation of the RET binding sites on OVA macromolecule. The adjustment of FI data to modified Scatchard model yielded the following results: n: 108 ± 16 and Ka: (7 ± 4) × 10^5 M^{-1}. According to this, one OVA monomeric unit is able to bind ~108 RET molecules with an appreciable affinity. However, complementary binding techniques should be applied in order to check complex stoichiometry.

(ii) For OVAn, the increase in RET concentration promoted a gradual decrease in RFI, and in the same way that OVA does, no shifts at maximum emission wavelength were registered (Fig. 1c). RFI values are shown in Fig. 1d, highlighting the phenomenon known as fluorescence quenching. Assuming a static quenching mechanism, RET molecules would bind nearly to Trp and/or Tyr residues, so emission fluorescence would be gradually reduced as a consequence of complex formation (Lakowicz, 2006). Therefore, the magnitude of RFI decrement could be proportional to OVAn-RET complex concentration in solution (Sponton et al., 2015b; Wang et al., 2013). Binding stoichiometry (n) and association constant (Ka) values were obtained as it was previously mentioned, yielding the following results: n_1: 16 ± 10 and Ka_1: (7 ± 2) × 10^4 M^{-1}, n_2:67 ± 9 and Ka_2: (2 ± 1) × 10^5 M^{-1}. According to Le Maux et al. (2013), these binding stoichiometry results were referred to OVA monomeric unit. Hence, it could deduced that one OVA monomeric unit in OVAn is able to bind ~83 RET molecules ($n_1 + n_2$) in two kinds of RET binding sites, being one of them of higher affinity (10^5 M^{-1}). The decrease in the total number of RET molecules bound per OVA monomeric unit could be explained taking into account that OVAn formation would require some hydrophobic patches on OVA molecules which could involve RET binding sites.

(iii) Differences in formation of OVA-RET and OVAn-RET complexes could be directly linked to protein conformational state. OVAn obtention process implicated denaturation/aggregation phenomena by means of heat treatment (Sponton et al., 2015b). This condition was above OVA denaturation temperature (~80.1 °C, according Matsudomi, Takahashi, and Miyata (2001)), which could result in significant conformational changes on native OVA. These changes can be deduced from OVA and OVAn fluorescence spectra (showed in Fig. 1a and c, respectively). The OVAn obtention caused a reduction of 28% OVA FI. This self-quenching phenomenon would promoted by hydrophobic interactions and disulphide bounds, and in general, it is consistent with the existence of

considerable conformational changes in the protein (Le Maux et al., 2013; Perez et al., 2014).

3.1.2. Extrinsic fluorescence

For getting some knowledge about the mode of binding of RET to proteins (OVA and OVAn), extrinsic fluorescence experiments were performed. Fig. 2a and c shows the effect of RET concentration (0–200 μM) on ANS fluorescence emission behaviour of OVA and OVAn, respectively. In order to gain a better understanding, RFI_{ANS} values were calculated and they were included in Fig. 2b and d. It was observed that:

(i) For OVA, the increase in RET concentration caused practically no differences in FI_{ANS}, and consequently, no significant changes in RFI_{ANS} values (Fig. 2a,b). Moreover, no shift at ANS maximum emission wavelength were observed (deduced from the insert in Fig. 2a), which suggests no change in the environmental polarity of ANS binding sites. These results are explained considering that a constant amount of ANS is bound to OVA possibly due to: (i) the probe binds to a particular hydrophobic domains on protein surface, different to RET binding sites, and/or (ii) ANS addition causes the RET displacement from the OVA surface.

(ii) For OVAn, the increase in RET concentration promoted a gradual decrease in FI_{ANS} and RFI_{ANS} (Fig. 2c and d). This behaviour could be interpreted considering an increasingly lower amount of OVAn-ANS complexes formed in solution. So, the number of available hydrophobic sites for binding ANS was decreased with RET concentration. Furthermore, there was a significant red shift at the ANS maximum emission wavelength (observed in the insert in Fig. 2c), which could suggest that the probe is bound in an increasingly polar environment. These results highlight that the mode of binding of RET to OVAn could respond to an inside-out saturation mechanism in which inner sites are firstly filled. A similar behaviour was recently reported by Sponton et al. (2016) for evaluation the mode of binding of linoleic acid (LA) to OVAn.

(iii) Differences in the mode of binding of RET to proteins (OVA and OVAn) could be directly linked with conformational changes involved in OVAn formation process. Heat treatment caused an increase of 7 folds OVA FI_{ANS} (as it can be observed in Fig. 2a and c), suggesting the existence of a great availability of hydrophobic patches for ANS binding, as a consequence of protein denaturation (Sponton et al., 2015a). Nevertheless, the increase in protein surface hydrophobicity did not cause an increase in RET binding ability, because

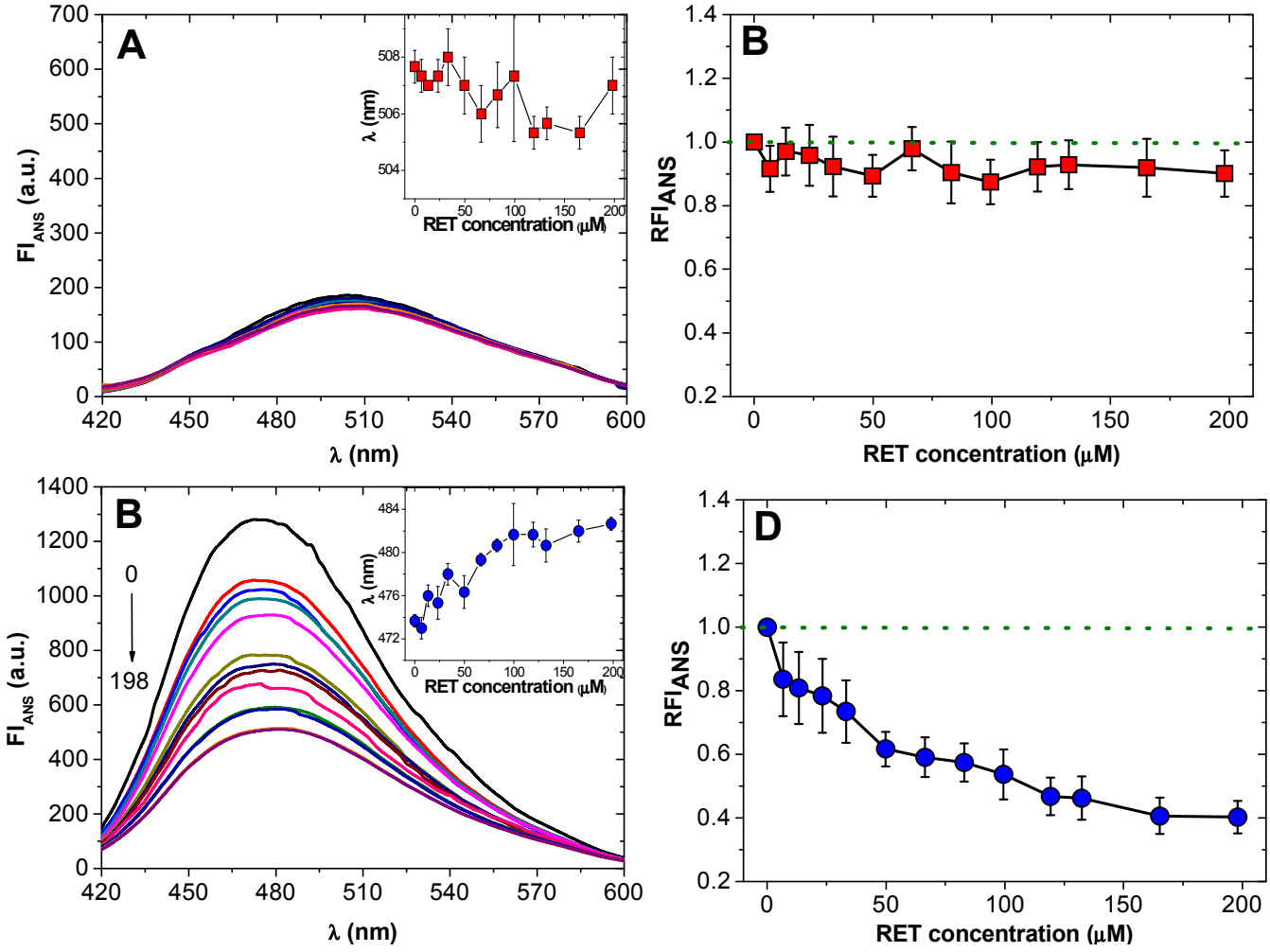

Fig. 2. Effect of retinol (RET) concentration (in the range 0–198 μM) on the ANS extrinsic fluorescence intensity (FI_{ANS}) for OVA (A) and OVAn (C); and on the ANS relative fluorescence intensity (RFI_{ANS}) for (■) OVA (B), and (●) OVAn (D). Inserts in (B) and (D) correspond to the wavelength (λ, nm) at the maximum FI_{ANS}. Conditions: Protein concentration: 1 μM, pH 7.0 (50 mM phosphate buffer), ANS concentration: 45 μM, Temperature: 20 °C. Values are showed as mean ± standard deviation.

OVAn attached a lower RET amount (in terms on monomeric unit) in comparison with OVA. This observation suggest that mechanism of RET binding to proteins seems to require certain specificity level at the binding sites (Le Maux et al., 2013; Perez et al., 2014).

3.2. Colloidal stability

3.2.1. Proteins

Colloidal stability of protein-ligand complexes could be strongly influenced by protein phase behaviour at different pH conditions. Hence, pH-dependent phase behaviour for pure OVA and OVAn was firstly examined considering absorbance as a measure of dispersion turbidity (Perez et al., 2015). Fig. 3a shows the effect of pH on the absorbance at 400 nm for OVA and OVAn dispersions. For OVA, the decrease in pH caused practically no changes in absorbance values and in dispersion visual appearances (Fig. 3c). However, for OVAn, the decrease in pH caused no modification in absorbance value up to about pH 6.0, from which it increased reaching a maximum at pH 5.0–4.5. Then, absorbance value decreased up to about pH 3.0, and remained constant up to pH 2.5. The high absorbance value for OVAn dispersion observed at pH 5.5–4.0 could be explained considering an increase in particle size as a consequence of a reduction in OVAn net charge. Reduced net charge usually promotes a decrease in electrostatic repulsion between proteins, so attractive colloidal interactions (e.g. van de Waals and hydrophobic forces) are enhanced, leading an increase in protein particle size by aggregation. This phenomenon could also explain OVAn sedimentation observed between pH 5.5–4.0 (Fig. 3d). Otherwise, this phenomenon could not occur for OVA dispersions possibly due to the smaller size of OVA macromolecule.

The pH value at which protein net charge is zero is known as isoelectric point (pI). In order to estimate the pI values for OVA and OVAn, ζ potential measurements at different pH values were performed, and results are shown in Fig. 3b. It was noted that pH decrement caused a reduction in the negative ζ potentials, reaching zero values at pH ~4.7. This pH value corresponds to pI estimation for both OVA and OVAn. Furthermore, the decrease in aqueous medium pH caused an increase in the positive ζ potentials for both proteins. In general, it could be concluded that pH-dependent charge profiles for OVA and OVAn were quite similar, suggesting that heat treatment virtually does not alter native OVA net charge. Results for OVAn would confirm that the decrease in protein net charge magnitude (derived from ζ potential values) could be responsible for the high absorbance values observed around pI. At these conditions, differences in colloidal stability of OVA and OVAn dispersions could be attributed to differences in particle sizes and conformational state of the proteins, native vs. denatured/aggregated, respectively.

3.2.2. Complexes

In agro-food sector, definition of nanosized materials is still not clear. So, particles with both, size strictly <100 nm and with few hundred nm could be defined as “nanoparticles” (Gutiérrez et al., 2013; Joye, Davidov-Pardo, & McClements, 2014). In general, it is well established that small particle sizes and high ζ potentials are requirements needed for obtaining high colloidal stability in food aqueous mediums (Lesmes & McClements, 2009; Perez et al., 2015). In this section, colloidal stability of OVA-RET and OVAn-RET complexes is analyzed taking into account PSD determination at pH values of 4.0 and 7.0 (chosen according to the results of protein colloidal stability discussed previously). Thus, the effect of pH on PSDi and PSDv for OVA-RET and OVAn-RET complexes is shown in Fig. 4. PSD results for pure OVA and OVAn were included as controls. It was observed that:

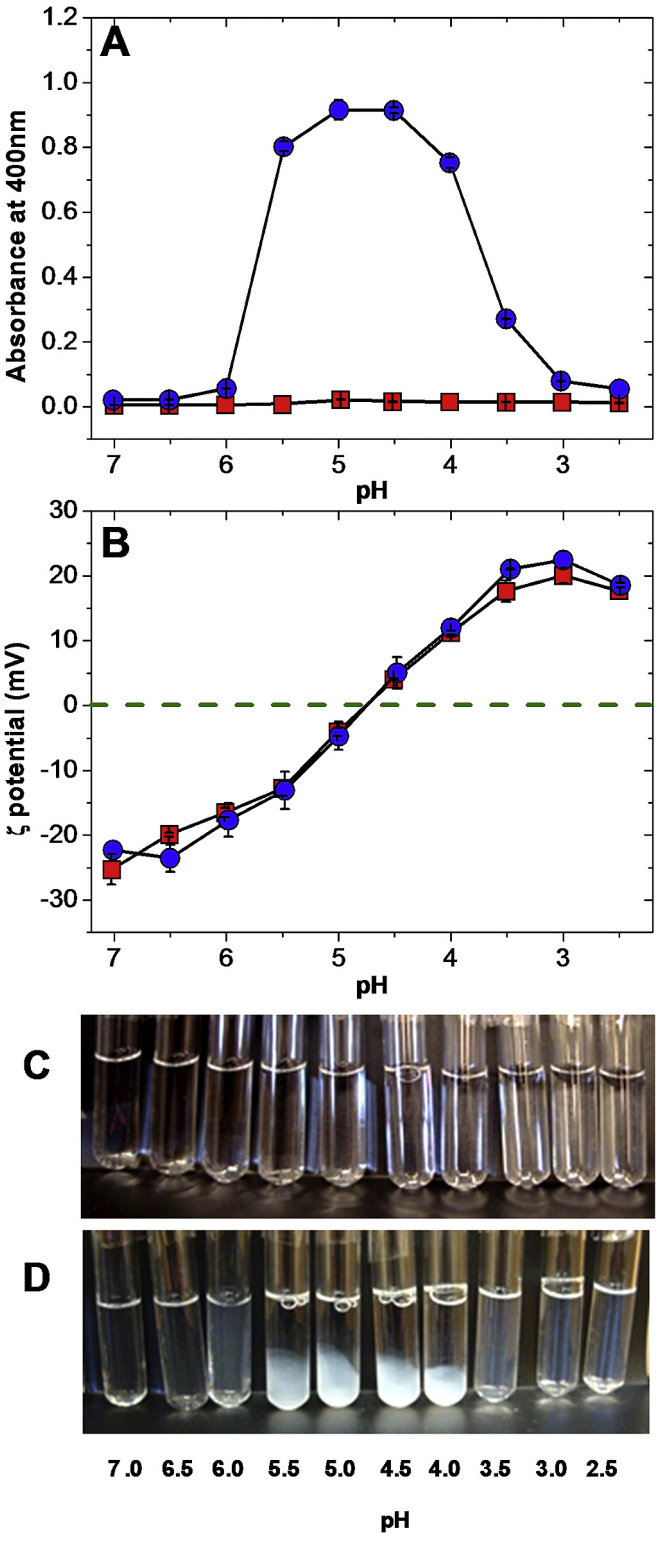

Fig. 3. Phase behaviour of pure proteins as a function of aqueous medium pH: Absorbance at 400 nm as a measure of system turbidity (A) and ζ potential (B) for (■) OVA and for (●) OVAn and visual appearance for OVA (C) and for OVAn (D). Conditions: Protein concentration: 23 μM. Values in (A) and (B) are showed as mean ± standard deviation.

(i) For pure OVA, at pH 4.0 two peaks in PSDi at 10 ± 1 and 61 ± 2 nm was observed (Fig. 4a); however, according to PSDv results these ones represented 92 and 8%, respectively

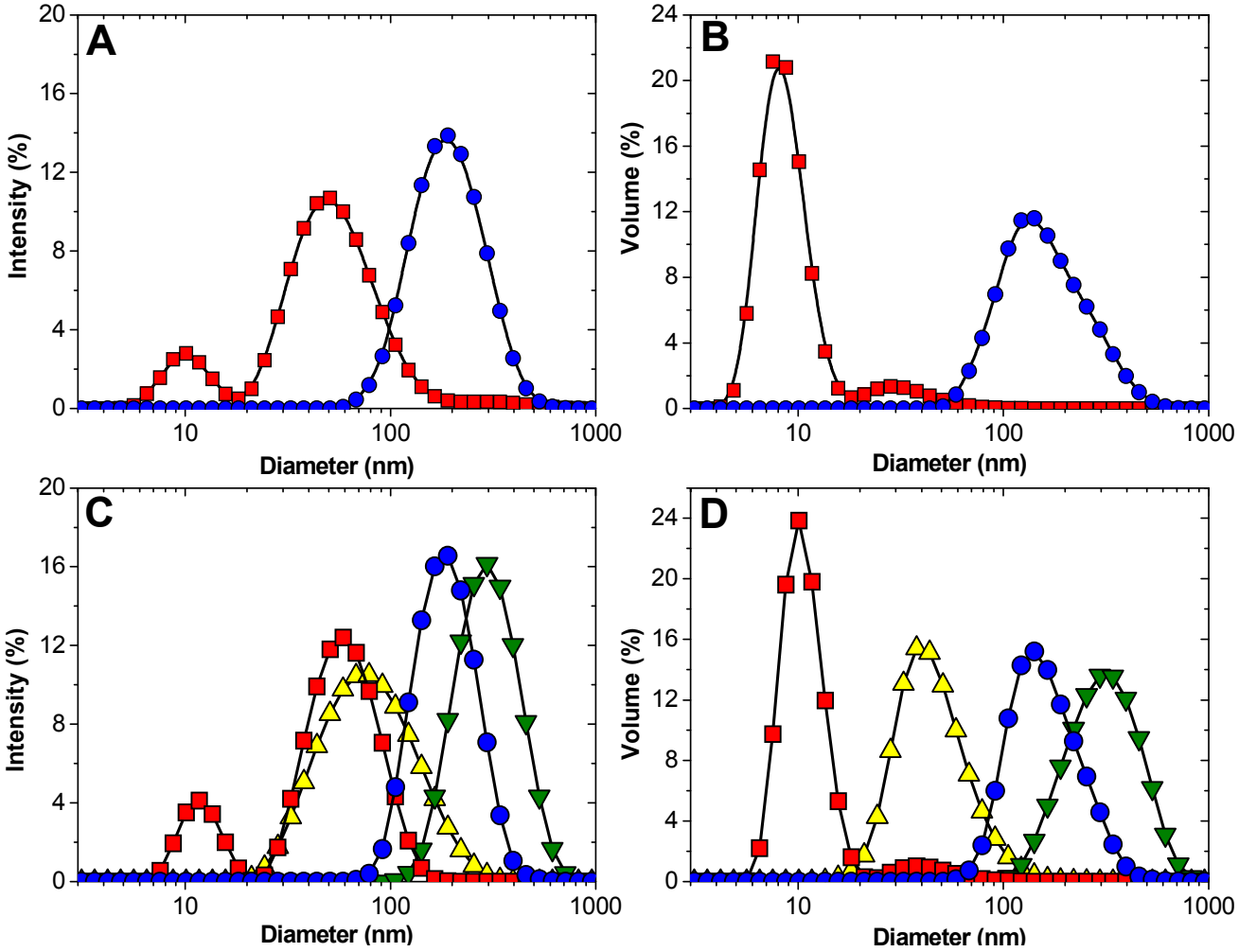

Fig. 4. Particle size distribution (PSD) based on Intensity and Volume percentage (%): (A) and (B): (■) OVA and (●) OVA-RET complex at pH 4.0; (C) and (D): (■) OVA (●), OVA-RET (▲), OVAn and (▼) OVAn-RET complex at pH 7.0. Conditions: Protein concentration: 23 μM, RET concentration: 2.3 mM, Temperature: 25 °C.

(Fig. 4b). At pH 7.0, a similar PSD behaviour was observed registering a first peak at 9 ± 1 nm (94%) and a second peak at 52 ± 2 nm (6%). Kang, Ryu, Park, Czarnik-Matusewicz, and Jung (2014) reported that no conformational changes in second and tertiary OVA structure are registered as a consequence of pH changes. Hence, in general terms, it could be concluded that first peaks observed for both pH values would correspond largely to OVA hydrodynamic diameter, and the second one to traces of some aggregated protein. For OVA-RET complexes, it was evident an increase in OVA size after RET complexation, being the complex hydrodynamic diameters of 203 ± 17 (92%) and 176 ± 4 nm (100%) at pH 4.0 and 7.0, respectively. The higher size of OVA-RET nanocomplex registered at pH 4.0 could be explained considering a decrease in the electrostatic repulsion between net charges. At this pH value, it was noted that RET complexation not alter significantly ζ potential of OVA ($p > 0.05$); whereas at pH 7.0 OVA-RET nanocomplexes showed a slight increase in ζ potential value in comparison with pure OVA (Table 1). In general, these results are in agreement with the hypothesis that colloidal stability of OVA-RET nanocomplexes is mainly governed by OVA electrical properties.

(ii) For OVAn and OVAn-RET complexes at pH 4.0, the PSD analysis was not possible to carry out due to the gradual particle sedimentation at the bottom of the measurement cell. However, as it can be observed in Fig. 4c and d, PSD analysis at pH 7.0 was performed yielding the following size data for OVAn and OVAn-RET complexes: 88 ± 1 nm (100%) and 312 ± 11 nm (100%), respectively. Regarding the electrical properties of OVAn-RET nanocomplexes, it can be deduced from Table 1 that complexation not modified significantly OVAn ζ potential value, suggesting that colloidal stability of OVAn-RET nanocomplexes is govern by aggregated protein behaviour.

Table 1
Effect of protein-RET complexation on ζ potential (mV) of OVA and OVAn as a function of aqueous medium pH. Conditions: Protein concentration: 23 μM, RET concentration: 2.3 mM, Temperature: 25 °C. Values are showed as mean standard deviation and different letters indicate statistical differences ($p < 0.05$).

pH	Systems	ζ Potential (mV)
4.0	OVA	$+11 \pm 0^{c}$
	OVA-RET	$+12 \pm 1^{c,d}$
	OVAn	$+12 \pm 1^{c,d}$
	OVAn-RET	$+14 \pm 0^{d}$
7.0	OVA	-21 ± 0^{b}
	OVA-RET	-25 ± 2^{a}
	OVAn	-25 ± 1^{a}
	OVAn-RET	-26 ± 2^{a}

3.3. Retinol photochemical stability

Usually, light and oxygen promote RET decomposition via formation of inactive metabolite species in close dependence of environmental conditions (Failloux et al., 2004). Therefore, the hypothesis that RET vehiculization under the form of nanocomplexes could prevent its deterioration against light and dissolved oxygen (DO) is discussed in this section. For this, a photochemical decomposition assay was performed at pH 4.0 and 7.0 over 30 h examination. The effect of aqueous medium pH on RET photochemical decomposition (%) for OVA-RET and OVAn-RET nanocomplexes is shown in Fig. 5. Moreover, initial DO concentrations are reported in Table 2. Results are discussed as follow:

(i) For $RET_{darkness}$ and RET_{light} controls, RET decomposition linearly increased up to 9 h. Then, for $RET_{darkness}$ control, the quantity of deteriorated RET practically did not increase up to 30 h examination (17.0 ± 1.0%), whereas for RET_{light} control, decomposition progressed at a lower rate up to reach 33.0 ± 1.0%. For these controls, the same initial DO content should be considered (4.1 ± 0.0 mg DO/L). Therefore, it can be deduced that up to 9 h, RET decomposition would be controlled by DO, and then the catalytic effect of light could be observed (Failloux et al., 2004).

(ii) For OVA-RET nanocomplexes at pH 4.0 (Fig. 5a), it was observed that RET decomposition was similar to RET_{light} up to about 24 h, from which a less pronounced RET decomposition took place up to reach 27.1 ± 0.2%. This result suggest that slight RET protective effect (from 24 h examination) is mainly due to the complexation with OVA. On the other hand, decomposition profile for OVA-RET nanocomplexes at pH 7.0 is shown in Fig. 5b. It was noted an increase in RET decomposition over the whole testing period up to reach 39.7 ± 0.7% at 30 h examination. A possible explanation lies in the largest surface area/volume ratio (smallest size) of OVA-RET complexes at pH 7.0 in comparison with the ones at pH 4.0 (Fig. 4), which could promote a greater accessibility to photochemical deterioration factors. Moreover, the lowest electrostatic repulsion between OVA-RET nanocomplexes at pH 4.0 (which lead to largest particle size) could favor RET photochemical stability. Thus, it would seem that factors controlling OVA-RET colloidal behaviour could also play a role in RET photochemical stability.

(iii) For OVAn-RET nanocomplexes at pH 7.0 (Fig. 5b), an increase was observed in RET decomposition with respect to controls at short times, suggesting that some RET molecules exposed onto OVAn surface are firstly deteriorated. Then, decomposition profile was similar to RET_{light} control up to 18 h examination, from which a significant reduction in RET decomposition was noted (23.3 ± 0.4%).

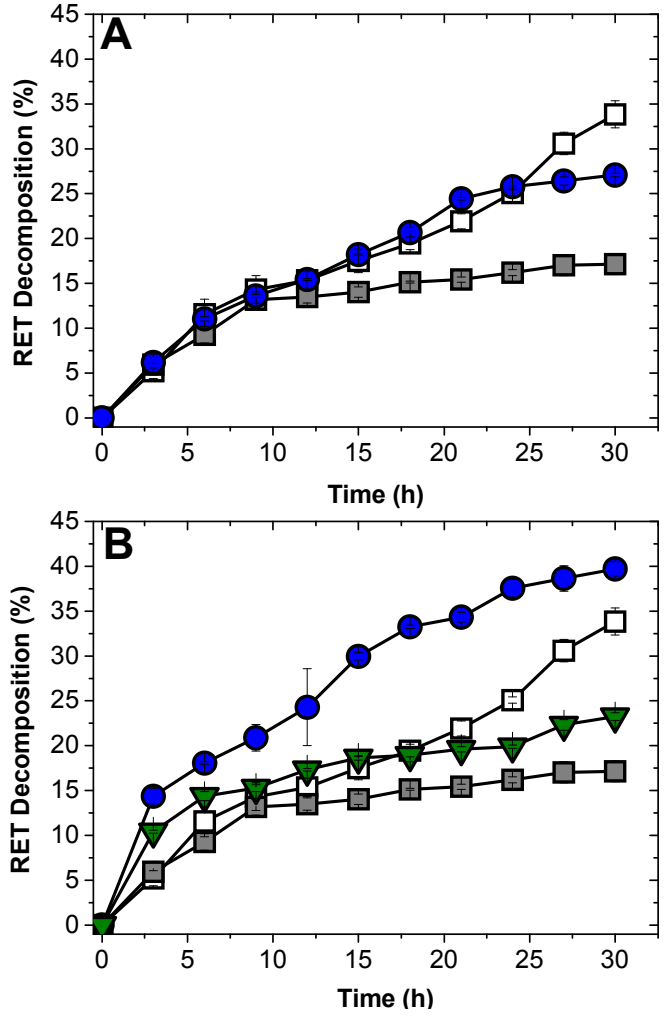

Fig. 5. Retinol (RET) photochemical decomposition (%) as a function of time (h): (A) OVA-RET complex (●) at pH 4.0; (B) OVA-RET complex (●) and OVAn-RET complex (▼) at pH 7.0. Controls: (■) pure RET in darkness (RET_{dark}), (□) pure RET in light (RET_{light}). Conditions: Protein concentration: 6.7 μM, RET concentration: 670 μM, Temperature: 25 °C. Experiments were performed using a fluorescent lamp (BAW, 65 W, 750 lm, 6400 K), with exception of RET_{dark} control. Values are showed as mean ± standard deviation.

Table 2
Initial dissolved oxygen concentration (DO mg/L) and retinol (RET) photochemical decomposition (%) at 30 h for 50 mM phosphate buffer, OVA pH 4, OVA pH 7 and OVAn pH 7. Conditions: Protein concentration: 6.7 μM, RET concentration: 670 μM, Temperature: 25 °C. Values are showed as mean standard deviation and different letters indicate statistical differences ($p < 0.05$).

Systems	RET photochemical decomposition at 30 h	DO (mg/L)
Buffer	33 ± 1^{c}	$4{,}1 \pm 0^{b}$
OVA pH 4	$27{,}1 \pm 0{,}2^{b}$	$3{,}9 \pm 0{,}1^{a}$
OVA pH 7	$39{,}7 \pm 0{,}7^{d}$	$5{,}4 \pm 0{,}2^{c}$
OVAn pH 7	$23{,}3 \pm 0{,}4^{a}$	$4{,}1 \pm 0{,}1^{b}$

In the case of OVA-RET pH 7, a significant higher DO content was obtained respect to RET controls ($p < 0.05$), Hence, the increased DO content in this system could explain the greater RET decomposition observed. However, as can be observed in Table 2, there is not a clear relation between RET photochemical decomposition and DO concentration, highlighting that observed RET protective effect would be mainly attributed to the complexation with OVAn. For example, from a comparison between RET decomposition and DO concentration values for OVA pH 4.0 and OVAn pH 7.0, the greater RET decomposition did not correspond to the grater DO concentration.

It is clearly evident that OVAn-RET nanocomplexes were more effective than OVA-RET nanocomplexes for RET photochemical stability preservation. This finding could be interpreted in terms of special mode of RET binding, which derive from the denatured/aggregated state of OVAn. Although the complete RET photochemical preservation was not reached with OVA-RET (at pH 4.0) and OVAn-RET nanocomplexes (at pH 7.0), a stability improvement could be achieved by adding a polysaccharide cover onto nanocomplexes surface (Perez et al., 2015; Zimet & Livney, 2009). This hypothesis will be addressed in a forthcoming paper.

4. Conclusions

Results derived from this research allowed to conclude that RET binding properties of OVA were strongly dependent on protein aggregation. It was highlighted that aggregated OVA (OVAn) was able to bind a lower RET amount in comparison with OVA, possibly due to its formation (mediated by hydrophobic interactions and disulphide bonds) could involve some hydrophobic sites needed for binding RET. Besides, the colloidal stability of RET complexes, particle sizes and electrical properties were influenced by OVA aggregation. All these factors seemed to play an important and a particular role in the preservation of RET photochemical stability in aqueous mediums. In the case of OVA-RET nanocomplexes, aqueous medium pH (pH 4.0 or 7.0) was critical for RET photochemical stability; whereas in the case of OVAn-RET nanocomplexes, its special mode of binding, was determinant of an increased RET preservation at pH 7.0. Finally, nanocomplexes formed with OVAn promoted a higher RET photochemical stability than the ones formed with OVA. These findings could be of practical interest in the formulation of RET-fortified foods.

Acknowledgments

Authors acknowledge the financial support of the following projects: CAI+D-2013-50120110100-171-LI (UNL) and PICT-2014-2636 (ANPCyT), CONICET for the PhD fellowships awarded to Flavia F. Visentini and Osvaldo E. Sponton, and especially to Lic. Alicia Guibert from Centro Universitario Reconquista Avellaneda (UNL, Santa Fe, Argentina) for the kindness of supplying the materials for DO determination.

References

Allwood, M. C., & Plein, J. H. (1986). The wavelength-dependent degradation of vitamin A exposed to ultraviolet radiation. *International Journal of Pharmaceutics, 31*, 1–7.

Blayo, C., Marchal, S., Lange, R., & Dumay, E. (2014). Retinol binding to β-lactoglobulin or phosphocasein micelles under high pressure: Effects of isostatic high-pressure on structural and functional integrity. *Food Research International, 55*, 324–335.

Carlotti, M. E., Rossatto, V., & Gallarate, M. (2002). Vitamin A and vitamin A palmitate stability over time and under UVA and UVB radiation. *International Journal of Pharmaceutics, 240*, 85–94.

Castenmiller, J. J., & West, C. E. (1998). Bioavailability and bioconversion of carotenoids. *Annual Review of Nutrition, 18*, 19–38.

Cogan, U., Kopelman, S., & Shinitzky, M. (1976). Binding affinities of retinol and related compounds to retinol binding proteins. *European Journal of Biochemistry, 65*(1), 71–78.

Croguennec, T., Renault, A., Beaufils, S., Dubois, J., & Pezennec, S. (2007). Interfacial properties of heat-treated ovalbumin. *Journal of Colloid and Interface Science, 31*, 627–636.

Failloux, N., Bonnet, I., Perrier, E., & Baron, M. E. (2004). Effects of light, oxygen and concentration on vitamin A. *Journal of Raman Spectroscopy, 35*, 140–147.

Frapin, D., Dufour, E., & Haertle, T. (1993). Probing the fatty acid binding site of β-lactoglobulins. *Journal of Protein Chemistry, 12*(4), 443–449.

Gutiérrez, F. J., Albillos, S. M., Casas-Sanz, E., Cruz, Z., García-Estrada, C., & García-Guerra, A. (2013). Methods for the nanoencapsulation of β-carotene in the food sector. *Trends in Food Science & Technology, 32*, 73–83.

Hattori, M., Watabe, A., & Takahashi, K. (1995). β-Lactoglobulin protects β-ionone related compounds from degradation by heating, oxidation, and irradiation. *Bioscience, Biotechnology, and Biochemistry, 59*(12), 2295–2297.

Hwang, Y. J., Oh, C., & Oh, C. G. (2005). Controlled release of retinol from silica particles prepared in O/W/O emulsion: The effects of surfactants and polymers. *Journal of Controlled Release, 106*, 339–349.

Jenning, V., & Gohla, S. H. (2001). Encapsulation of retinoids in solid lipid nanoparticles (SLN1). *Microencapsulation, 18*(2), 149–158.

Joye, I. J., Davidov-Pardo, G., & McClements, D. J. (2014). Nanotechnology for increased micronutrient bioavailability. *Trends in Food Science & Technology, 40*(2), 168–182.

Kang, D., Ryu, S. R., Park, Y., Czarnik-Matusewicz, B., & Jung, Y. M. (2014). pH-induced structural changes of ovalbumin studied by 2D correlation IR spectroscopy. *Journal of Molecular Structure, 1069*, 299–304.

Kontopidis, G., Holt, C., & Sawyer, L. (2002). The ligand-binding site of bovine betalactoglobulin: Evidence for a function? *Journal of Molecular Biology, 318*, 1043–1055.

Lakowicz, J. R. (2006). *Principles of fluorescence spectroscopy* (3rd ed.). Singapore/USA: Springer.

Le Maux, S., Bouhallab, S., Giblin, L., Brodkorb, A., & Croguennec, T. (2013). Complexes between linoleate and native or aggregated b-lactoglobulin: Interaction parameters and in vitro cytotoxic effect. *Food Chemistry, 141*, 2305–2313.

Lee, S. C., Yuk, H. G., Lee, D. H., Lee, K. E., Hwang, Y. I., & Ludescher, R. D. (2002). Stabilization of retinol through incorporation into liposomes. *Journal of Biochemistry and Molecular Biology, 35*(4), 358–363.

Lesmes, U., & McClements, D. J. (2009). Structure–function relationships to guide rational design and fabrication of particulate food delivery systems. *Trends in Food Science & Technology, 20*(10), 448–457.

Loveday, S. M., & Singh, H. (2008). Recent advances in technologies for vitamin A protection in foods. *Trends in Food Science and Technology, 19*, 657–668.

Matsudomi, N., Takahashi, H., & Miyata, T. (2001). Some structural properties of ovalbumin heated at 80 °C in the dry state. *Food Research International, 34*(2–3), 229–235.

Muresan, S., van der Bent, A., & de Wolf, F. A. (2001). Interaction of β-lactoglobulin with small hydrophobic ligands as monitored by fluorometry and equilibrium Dialysis: Nonlinear quenching effects related to protein-protein association. *Journal of Agricultural Food Chemistry, 49*, 2609–2618.

Nisbet, A. D., Saundry, R. H., Moir, A. J. G., Fothergill, L. A., & Fothergill, J. E. (1981). The complete amino-acid sequence of hen ovalbumin. *European Journal of Biochemistry, 115*, 335–345.

Noy, N. (2000). Signaling by retinol and its serum binding protein. Prostaglandins. *Leukotrienes and Essential Fatty Acids, 93*, 3–7.

Perez, A. A., Andermatten, R. B., Rubiolo, A. C., & Santiago, L. G. (2014). Beta-lactoglobulin heat-induced aggregates as carriers of polyunsaturated fatty acids. *Food Chemistry, 158*(1), 66–72.

Perez, A. A., Carrera Sánchez, C., Rodríguez Patino, J., Rubiolo, A., & Santiago, L. G. (2012). Effect of enzymatic hydrolysis and polysaccharide addition on the β-lactoglobulin adsorption at the air–water interface. *Journal of Food Engineering, 109*(4), 712–720.

Perez, A. A., Sponton, O. E., Andermatten, R. B., Rubiolo, A. C., & Santiago, L. G. (2015). Biopolymer nanoparticles designed for polyunsaturated fatty acid vehiculization: Protein-polysaccharide ratio study. *Food Chemistry, 188*, 543–550.

Puyol, P., Perez, M. D., Ena, J. M., & Calvo, M. (1991). Interaction of bovine β-lactoglobulin and other bovine and human whey proteins with retinol and fatty acids. *Agricultural and Biological Chemistry, 55*(10), 2515–2520.

Rice, E., Baird, R., Eaton, A. D., & Clesceri, L. S. (2012). *Standard Methods for the examination of water and wastewater* (22nd ed.). Washington D.C.: American Public Health Association; American Water Works Association & Water Environment Federation.

Shimoyamada, M., Yoshimura, H., Tomida, K., & Watanabe, K. (1996). Stabilities of bovine β-lactoglobulin/retinol or retinoic acid complexes against tryptic hydrolysis, heating and light-induced oxidation. *Lebensmittel Wissenschaft and Technology, 29*, 763–766.

Sommer, A., & Davidson, F. R. (2002). Assessment and control of vitamin A deficiency: The Annecy accords. *The Journal of Nutrition, 132*(9S), 2845–2849.

Sponton, O. E., Perez, A. A., Carrara, C. R., & Santiago, L. G. (2014). Effect of limited enzymatic hydrolysis on linoleic acid binding properties of β-lactoglobulin. *Food Chemistry, 146*, 577–582.

Sponton, O. E., Perez, A. A., Carrara, C. R., & Santiago, L. G. (2015a). Impact of environment conditions on physicochemical characteristics of ovalbumin heat-induced nanoparticles and on their ability to bind PUFAs. *Food Hydrocolloids, 48*, 165–173.

Sponton, O. E., Perez, A. A., Carrara, C. R., & Santiago, L. G. (2015b). Linoleic acid binding properties of ovalbumin nanoparticles. *Colloids and Surfaces, B: Biointerfaces, 128*, 219–226.

Sponton, O. E., Perez, A. A., Carrara, C. R., & Santiago, L. G. (2016). Complexes between linoleic acid and ovalbumin nanoparticles: Stoichiometric, kinetic and thermodynamic aspects. *Food Chemistry, 211*, 819–826.

Stephensen, C. V. (2001). Vitamin A, infection, and immune function. *Annual Review of Nutrition, 21*, 167–192.

Sun, H., & Kawaguchi, R. (2011). The membrane receptor for plasma retinol binding protein, a new type of cell-surface receptor. *International Review of Cell and Molecular Biology, 288*, 1–41.

Vilanova, N., & Solans, C. (2014). Vitamin A Palmitate–b-cyclodextrin inclusion complexes: Characterization, protection and emulsification properties. *Food Chemistry, 175*, 529–535.

Wang, Q., Allen, J. C., & Swaisgood, H. E. (1999). Binding of lipophilic nutrients to β-lactoglobulin prepared by bioselective adsorption. *Journal of Dairy Science, 82*, 257–264.

Wang, R. Q., Yin, Y. J., Li, H., Wang, Y., Pu, J. J., Wang, R., et al. (2013). Comparative study of the interactions between ovalbumin and three alkaloids by spectrofluorimetry. *Molecular Biology Reports, 40*, 3409–3418.

van de Weert, M., & Stella, L. (2011). Fluorescence quenching and ligand binding: A critical discussion of a popular methodology. *Journal of Molecular Structure, 998*, 144–150.

Weijers, M., & Visschers, R. W. (2002). Light scattering study of heat-induced aggregation and gelation of ovalbumin. *Macromolecules, 35*, 4753–4762.

Zimet, P., & Livney, Y. D. (2009). Beta-lactoglobulin and its nanocomplexes with pectin as vehiclesfor ω-3 polyunsaturated fatty acids. *Food Hydrocolloids, 23*, 1120–1126.